Antibacterial and Cellular Response of BBG - based Composites

This chapter discusses the effect of incorporation of piezoelectric BT/ NKN as secondary phase in borate bioglass on it's antibacterial and cellular response. In addition, the effect of surface polarization on antibacterial and cellular response has also been examined. The formation of pure phase BBG and their composites has been examined using X-ray diffraction analyses. The quantitative and qualitative analyses for both, the antibacterial and cellular response have been performed to examine the detailed in-vitro response of the developed composites. The mechanisms for antibacterial and cellular response on BBG and their composites have also been discussed elaborately.

6.1. Phase evolution

The X- ray diffraction (XRD) patterns of sintered BBG, BBG-30 vol. % NKN and BBG-30 vol. % BT composites are represented in Fig. 6.1. The XRD patterns were analyzed using X-pert high score software and indexed as per the standard JCPDS data. The XRD patterns reveal the formation of single phase of BBG (monoclinic), NKN (monoclinic) and BT (tetragonal). In case of composite samples, characteristic peaks of BBG, NKN and BT were observed without any reaction between the constituent phases.
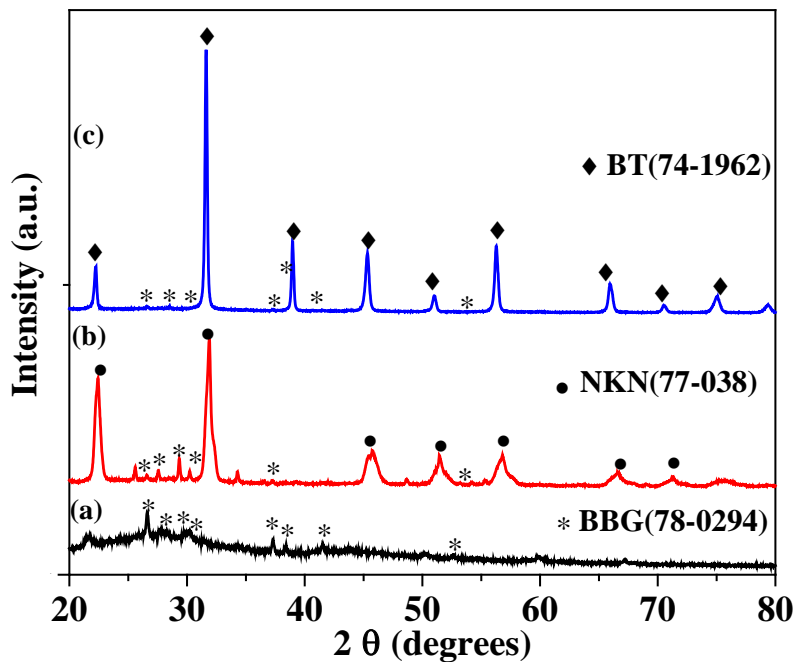
Fig. 6.1. The XRD patterns for sintered (a) BBG, (b) BBG-30 vol. % NKN and (c) BBG-30 vol. % BT composites.

6.2. *In-vitro* antibacterial response

6.2.1. MTT assay

The quantitative assessment of antibacterial response for *E. coli* and *S. aureus* bacteria, cultured on BBG and BBG-x NKN/BT (x = 30 vol.%) composites are represented in Fig. 6.2. The statistical analyses reveal that the developed BBG and BBG-NKN/BT composite samples demonstrate significant reduction in viability of *E. coli* bacteria, as compared to control sample [represented as (*) in Fig 6.2 (a)]. However, for *S. aureus* bacteria, the unpolarized and polarized BBG and BBG-30 vol. % NKN/BT composites demonstrate significant reduction in viability [represented as (*) in Fig 6.2 (b)]. It is clearly observed that incorporation of piezoelectric NKN and BT as secondary phases in BBG significantly

159

increases the antibacterial response for both, *E. coli* and *S.aureus* bacteria. The optical density, measured for both, *E. coli* and *S.aureus* bacteria significantly reduced on unpolarized and polarized BBG, BBG-30 NKN/BT composites, while compared with unpolarized BBG [represented as (**) in Fig 6.2]. In addition, the surface polarization also affects the antibacterial response of BBG and its composites. The negatively polarized surfaces of BBG, BBG-30 NKN/BT composites illustrate significant reduction in optical density of *E. coli* bacteria. However, for *S.aureus* bacteria, positively polarized surfaces of BBG, BBG-30 NKN/BT composites demonstrate significant reduction in optical density. It is clearly observed that the optical density of *E. coli* bacteria significantly reduces on polarized BBG-30 NKN/BT samples [represented as (#) in Fig 6.2 (a)] as compared to negatively polarized BBG. However, for *S.aureus* bacteria, all the developed samples show significant difference in optical density, except BBG-30 BT [represented as (#) in Fig 6.2 (b)], as compared to negatively polarized BBG. On the other hand, the optical density of *E. coli* bacteria reduces significantly on unpolarized and polarized BBG-30 NKN/BT composites [represented as (##) in Fig 6.2 (b)] as compared to positively polarized BBG. However, for *S.aureus* bacteria, the optical density reduces significantly on polarized BBG-30 NKN/BT composites [represented as (##) in Fig 6.2 (b)]. Overall, the MTT results demonstrate that incorporation of NKN/BT as secondary phase as well as polarization increases the antibacterial behavior of BBG and its composites.
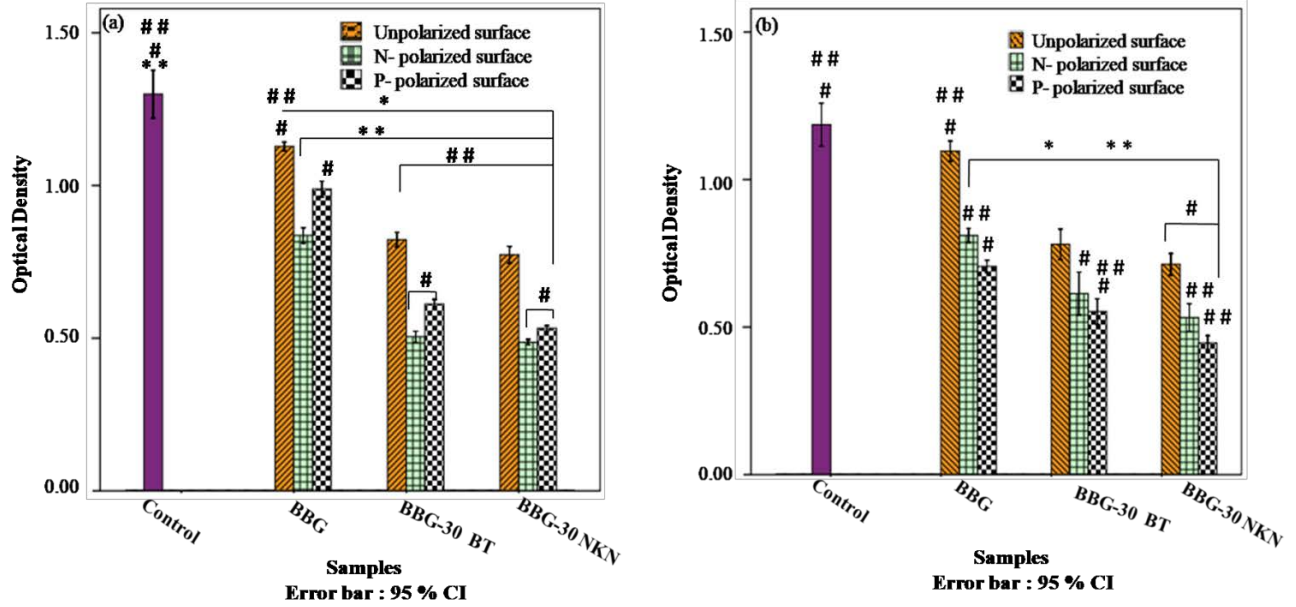
Fig. 6.2. The antibacterial response (MTT assay) of (a) E. coli and (b) S.aureus bacteria, cultured on unpolarized and polarized BBG-x NKN/BT (x = 30 Vol. %). The symbols (*) and (**) represent the statistically significant difference among all the samples with respect to control sample (glass cover slip) and unpolarized BBG respectively, at p < 0.05. The symbols (#) and (##) represent the statistically significant difference among all the samples with respect to N- polarized and P-polarized BBG, respectively, at p < 0.05.

6.2.2. Live/dead ratio

Live/dead ratio measures the ratio of viability of live to dead cells using the absorbance, measured in MTT assay. The percentage of viable cells were calculated as,

$$\textbf{Viability } (\%) = \frac{\textbf{mean absorbance of the samples}}{\textbf{mean absorbance of control}} \times \textbf{100} \qquad (\textbf{6.1})$$

The live/dead ratio for both, the bacteria, was calculated as,

$$\textbf{live/dead ratio} = \frac{\textbf{Live cells } (\textbf{viability } \%)}{\textbf{1} - \textbf{live cells } (\textbf{ viability } \%)} \qquad (\textbf{6.2})$$

161

Fig. 6.3 represents the live/dead ratio for *E. coli* and *S.aureus* bacteria, cultured on unpolarized and polarized BBG-x NKN/BT (x = 30 vol. %) composite samples. The incorporation of piezoelectric NKN/BT as secondary phase in BBG reduces the live/ dead ratio for BBG-30 NKN/BT composites. The statistical analyses demonstrate that live/dead ratio for both, *E. coli* and *S.aureus* bacteria significantly decreases on unpolarized and polarized BBG-30 NKN/BT composites as compared to unpolarized BBG [represented as (*) in Fig 6.3)]. Irrespective of addition of piezoelectric NKN/BT secondary phases, polarized surfaces also demonstrate bacteria specific antibacterial response. The live/dead ratio for *E. coli* bacteria significantly reduced on negatively polarized surfaces. However, positively polarized surfaces demonstrate significant reduction in live/dead ratio for *S. aureus* bacteria. It is observed that negatively polarized BBG- 30 NKN sample demonstrates minimum (~ 1.58) live/dead ratio for *E. coli* bacteria. However, positively polarized BBG-30 NKN sample has minimum (~ 1.82) live/dead ratio for *S.aureus* bacteria. Overall, the addition of piezoelectric NKN/BT as secondary phase as well as polarization induced surface charge reduces the live /dead ratio for both, *E. coli* and *S. aureus* bacteria.
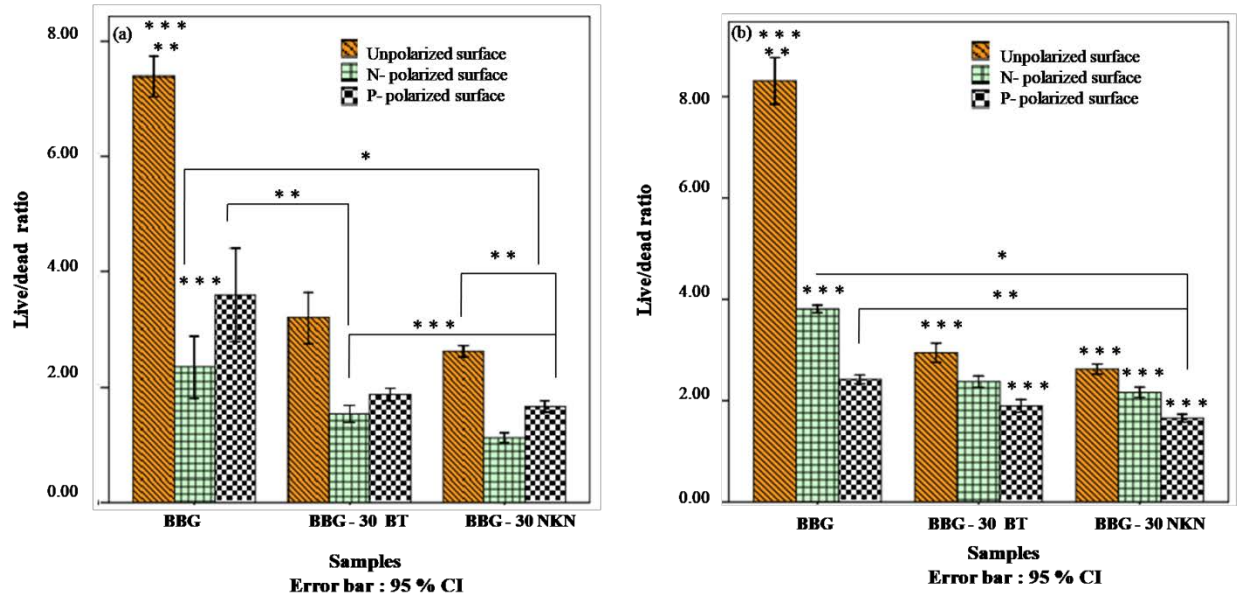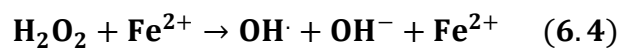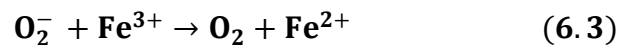
Fig. 6.3. Live/dead ratio for (a) E. coli and (b) S.aureus bacteria, while cultured on unpolarized and polarized BBG-x NKN/BT (x = 30 vol. %) composites. The symbol (*) represents the statistically significant difference among all the samples with respect to unpolarized BBG, at p < 0.05. The symbols (**) and (***) represent the statistically significant difference among all the samples with respect to N- polarized and P-polarized BBG, respectively, at p < 0.05.

6.2.3. Nitro blue tetrazolium (NBT) assay

The produced superoxide anions (reactive oxygen species) were quantified using NBT assay [1]. The unpolarized and polarized BBG-x NKN/BT (x = 30 vol. %) composite samples were cultured with *E. coli* and *S. aureus* bacteria. After required incubation period, 300 µl of NBT solution was added in the samples and incubated further for 1 h. The O^{2-} ions dilute NBT and produce a blue color precipitate (diformazan) which was dissolved in DMSO solution [2]. The absorbance of these dissolved diformazan was taken at 595 nm, which is directly proportional to the produced O^{2-} [36].

163

Fig. 6.4 represents the superoxide ions, produced on unpolarized and polarized BBG-x NKN/BT (x = 30 vol. %) composite samples, while cultured with *E. coli* and S. aureus bacteria. It is clearly observed that positively charged surfaces demonstrate higher superoxide production as compared to negatively polarized and unpolarized surfaces. The statistical analyses suggest that incorporation of piezoelectric NKN (30 vol. %) in BBG matrix increases the superoxide production significantly on unpolarized samples for both, *E. coli* and S. aureus bacteria. However, for addition of BT in BBG matrix, the superoxide production for both, the bacteria significantly increased on polarized surfaces only. The superoxide production for *E. coli* bacteria increased by about 48.32, 76.24 and 113.43 % on positively charged BBG, BBG-30 BT and BBG-30 NKN composite samples, respectively, while compared with unpolarized BBG. Similarly, for *S. aureus* bacteria, superoxide production was increased by about 72.45, 131.35, and 150.47 % on positively charged BBG, BBG-30 BT and BBG-30 NKN composite samples respectively, while compared with unpolarized BBG. It is observed that positively polarized surfaces are more prominent for generation of superoxide ions [3]. The polarized surfaces generate micro electric field which promote the ROS generation [4]. The produced ROS can damage the outer structure of bacterial cells as well as DNA and proteins. The electric field, generated by polarization disrupts the Fe- S clusters [5]. The damage of Fe- S clusters produces H_2O_2 indirectly through Fenton reaction (Eq. (6.3 and 6.4), these hydroxyl radicals can damage the DNA of bacterial cells [6].

$$O_2^- + Fe^{3+} \rightarrow O_2 + Fe^{2+} \qquad (6.3)$$

$$H_2O_2 + Fe^{2+} \rightarrow OH^. + OH^- + Fe^{2+} \qquad (6.4)$$

Overall, it can be concluded that positively polarized surfaces have higher superoxide production as compared to unpolarized and negatively polarized surfaces.
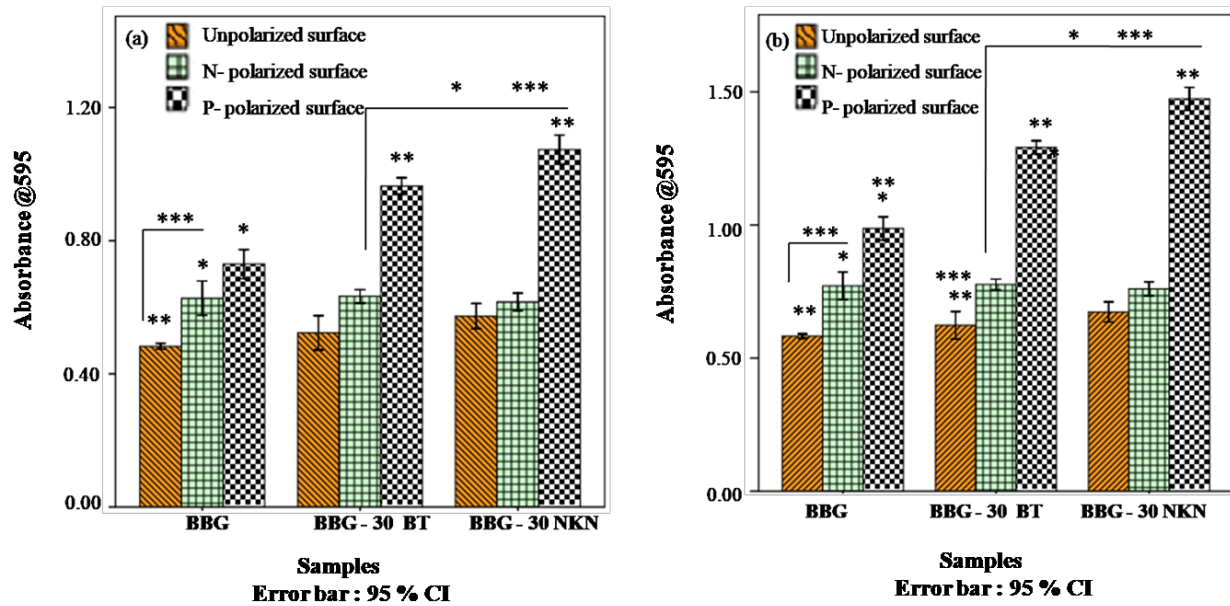

Fig. 6.4. Super oxide generation on unpolarized and polarized surfaces of BBG-x BT/ NKN (x = 30 vol. %) composites, while cultured with (a) E. coli and (b) S. aureus bacteria. The symbol (*) represents the statistically significant difference among all the samples with respect to unpolarized BBG at p < 0.05. The symbols (**) and (***) represent the statistically significant difference among all the samples with respect to N- polarized and P-polarized BBG, respectively, at p < 0.05.

6.2.4. Bacterial adhesion test

The adhesion of *E. coli* and *S.aureus* bacteria, cultured on BBG-x BT/ NKN (x = 30 vol. %) composites was observed using scanning electron microscopy. The sterile samples of unpolarized and polarized BBG-x BT/ NKN composites were seeded with 200 µl diluted (three fold serial dilution) bacterial strain and incubated for 12 h at 37 ˚C. The seeded samples were prepared for SEM. After incubation, the samples were washed thrice with phosphate buffer saline (1 x PBS). Following this, 0.25 % gluteraldehyde was added to fix

165

the cells on solid substrate. The samples were then incubated for 30 min at room temperature. The samples were again washed thrice with 1 x PBS. After this, the bacterial cells, adhered on the samples were dehydrated using ethanol series of 30 %, 50 %, 70%, 90 %, and 100 % for 10 minutes each. The samples were then dried and sputter coated with gold to examined under SEM (Zeiss, EVO 18 Research).

Fig. 6.5 represents the scanning electron microscopic images of *E. coli* bacteria, adhered on BBG-x BT/ NKN (x = 30 vol. %) composite samples. It is clearly observed that the addition of NKN/ BT as secondary phase in BBG matrix reduces the adhesion of *E. coli* bacteria [Fig 6.5 (a-e)]. Irrespective of addition of secondary phase, polarized surfaces also reduce the bacterial adhesion. The negatively polarized surfaces of all the developed compositions demonstrate lower adhesion of *E. coli* bacteria as compared to unpolarized and positively polarized surfaces [Fig.6.5 (d-f)]. However, positively polarized surfaces of all the compositions demonstrate lower bacterial adhesion as compared to unpolarized BBG [Fig 6.5 (g-i)]. The electrostatic interaction between negatively charged surface and *E. coli* bacteria (negatively charged) is responsible for lower adhesion of *E. coli* bacteria on negatively charged surfaces. The microscopic images of *E. coli* bacteria adhered on unpolarized and polarized surfaces of BBG-x BT/ NKN composite support the MTT assay results.
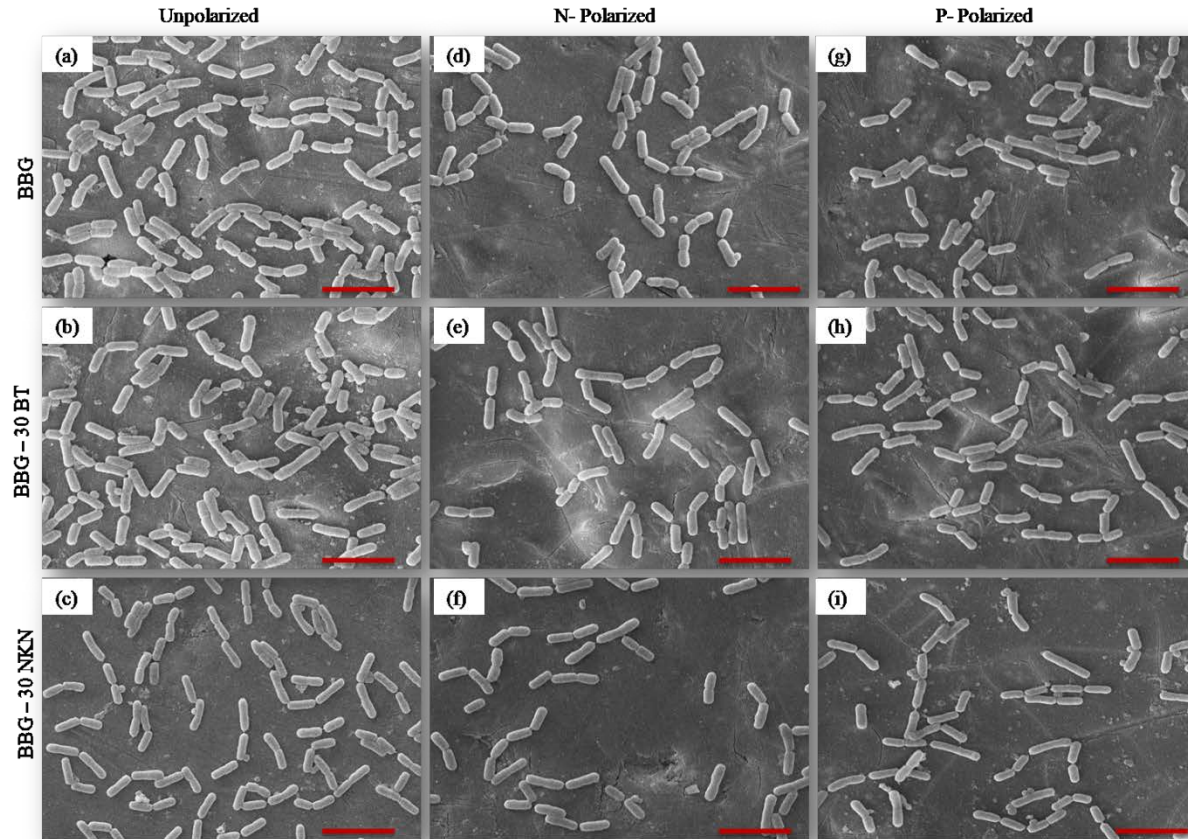
Fig. 6.5. The scanning electron microscopic images, demonstrating the adhesion of E. coli bacteria on unpolarized and polarized BBG-x BT/ NKN (x = 30 vol. %) composite sample surfaces (scale bar corresponds to 2 μm).

Fig. 6.6 represents the SEM micrographs of *S. aureus* bacteria, adhered on BBG-x BT/ NKN (x = 30 vol. %) composite samples. The adhesion of *S. aureus* bacteria depends upon incorporation of piezoelectric NKN/BT as secondary phase in BBG matrix. It is clearly observed that unpolarized surfaces of BBG-30 vol. % BT and BBG-30 vol. % NKN composite samples demonstrate lower adhesion of *S. aureus* bacteria, as compared to unpolarized BBG sample surface [Fig. 6.6 (a-c)]. In addition, the polarized surfaces of all the compositions reduce the bacterial adhesion as compared to unpolarized BBG sample.

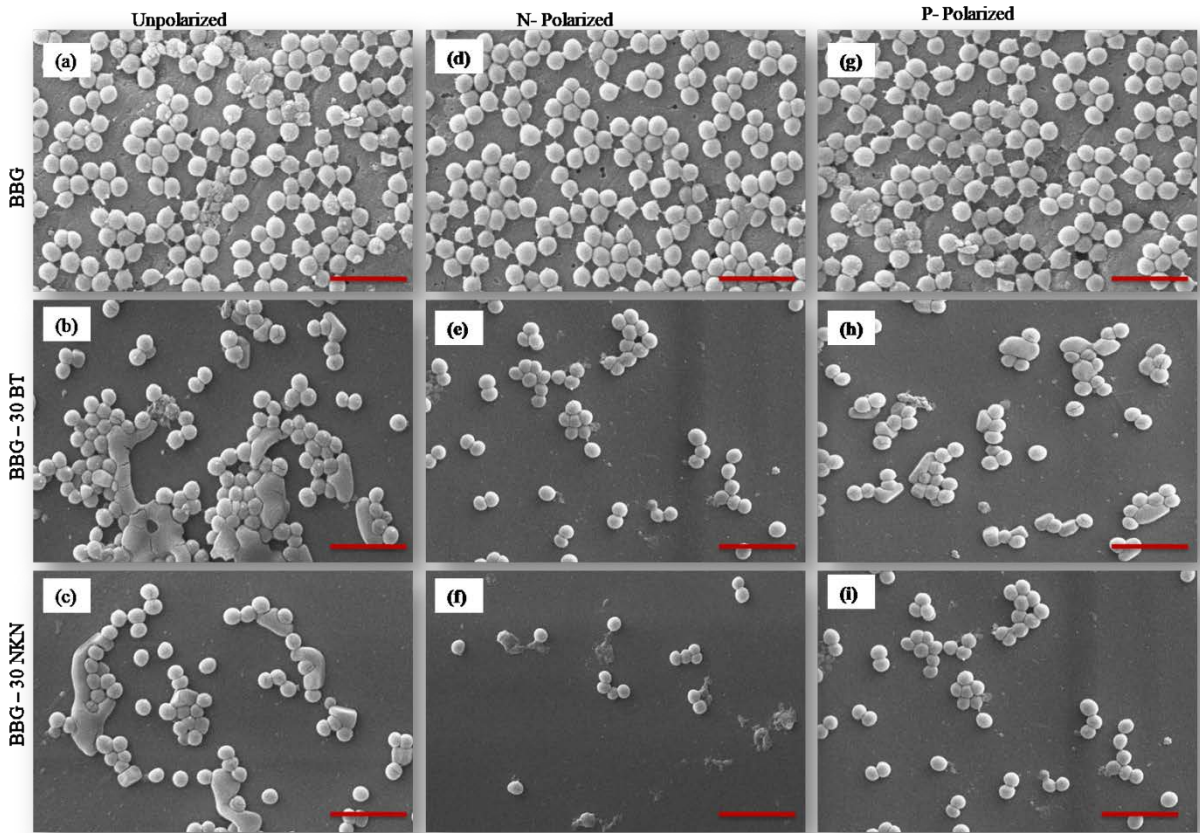The negatively polarized surfaces of all the compositions demonstrate lower adhesion of *S. aureus* bacteria.

Fig. 6.6. The scanning electron microscopic images, demonstrating the adhesion of S. aureus bacteria on unpolarized and polarized BBG-x BT/ NKN (x = 30 vol. %) composite sample surfaces (scale bar corresponds to 2 µm).

All the above mentioned results confirm that the incorporation of piezoelectric BT and NKN as the secondary phases in BBG matrix enhances the antibacterial behavior. However, it has been reported that BBG itself exhibits antibacterial nature due to the presence of network modifier elements such as Mg, K in BBG [7, 8]. It has been demonstrated that these network modifiers have the tendency to dissolve in the culture solution which alter the pH of the solution [9].

It has been demonstrated that the presence of borate (B_2O_3) in BBG can reduce the bacterial infection [10]. In addition, piezoelectric BT and NKN are known to be antibacterial and biocompatible materials [11]. Apart from incorporation of piezoelectric secondary phases, polarization induced surface charges are also responsible for such antibacterial response [12]. Outer membranes of the gram positive and gram negative bacterial cells possess lipopolysaccharides and peptidoglycan with negative charge [13]. The surface charge, induced by the polarization interact with cell membrane and repel the gram negative bacteria due to having more negative charge than gram positive bacterial cells [14]. On the other hand, positively charged surface neutralizes the negative charge of bacteria and alter the architecture of lipid layer by enhancing the permeability of cell membrane which consequently, damage the bacterial cells and lead to cell death [15]. Therefore, electrostatic interaction between charged surface and bacterial cell membranes is one of possible factors for such antibacterial behavior of BBG and BBG – BT/NKN composite samples [16,17]. The hydrophilicity of polarized surface can also be an influential factor for such type of antibacterial behavior [18]. It has been reported that polarization increases the hydrophilicity of surfaces; such surfaces resist the bacterial adhesion [19].

6.3. Cell culture study

In-vitro cellular response of prepared compositions was observed using human osteoblast like MG-63 cells. The quantitative analyses were done using MTT assay whereas, qualitative analyses were done by taking fluorescence microscopic images of cells, adhered on prepared sample surfaces.

6.3.1. MTT assay

Fig. 6.7 represents the viability of MG-63 cells in terms of optical density, after 3, 5 and 7 days of incubation. The viability of MG-63 cells increases with addition of piezoelectric secondary phase in BBG matrix up to 7 days of culture.

The polarization of developed sample surfaces also favors the proliferation of MG-63 cells after incubation of up to 7 days. The statistical analyses reveal that the optical densities of all the samples, expect unpolarized BBG demonstrate significant enhancement as compared to control sample, after 3, 5, and 7 days of incubation [represented as (*) in Fig. (6.7)]. In addition, the negatively polarized surfaces of all the compositions illustrate higher proliferation of MG-63 cells after 3, 5 and 7 days of culture, as compared to unpolarized and positively polarized sample surfaces of respective composition and culture periods. The viability of MG-63 cells on negatively polarized BBG, BBG-30 vol. % BT and BBG-30 vol. % NKN composites are calculated to be about (43, 109, 131%) (81, 130, 178 %) and (181, 252, 304 %) after 3, 5, and 7 days of incubation respectively, as compared with unpolarized BBG sample, after 3 days of incubation. Overall, it is observed that viability of MG-63 cells increases with incubation period, addition of piezoelectric BT/ NKN as secondary phase as well as polarization induced surface charge.
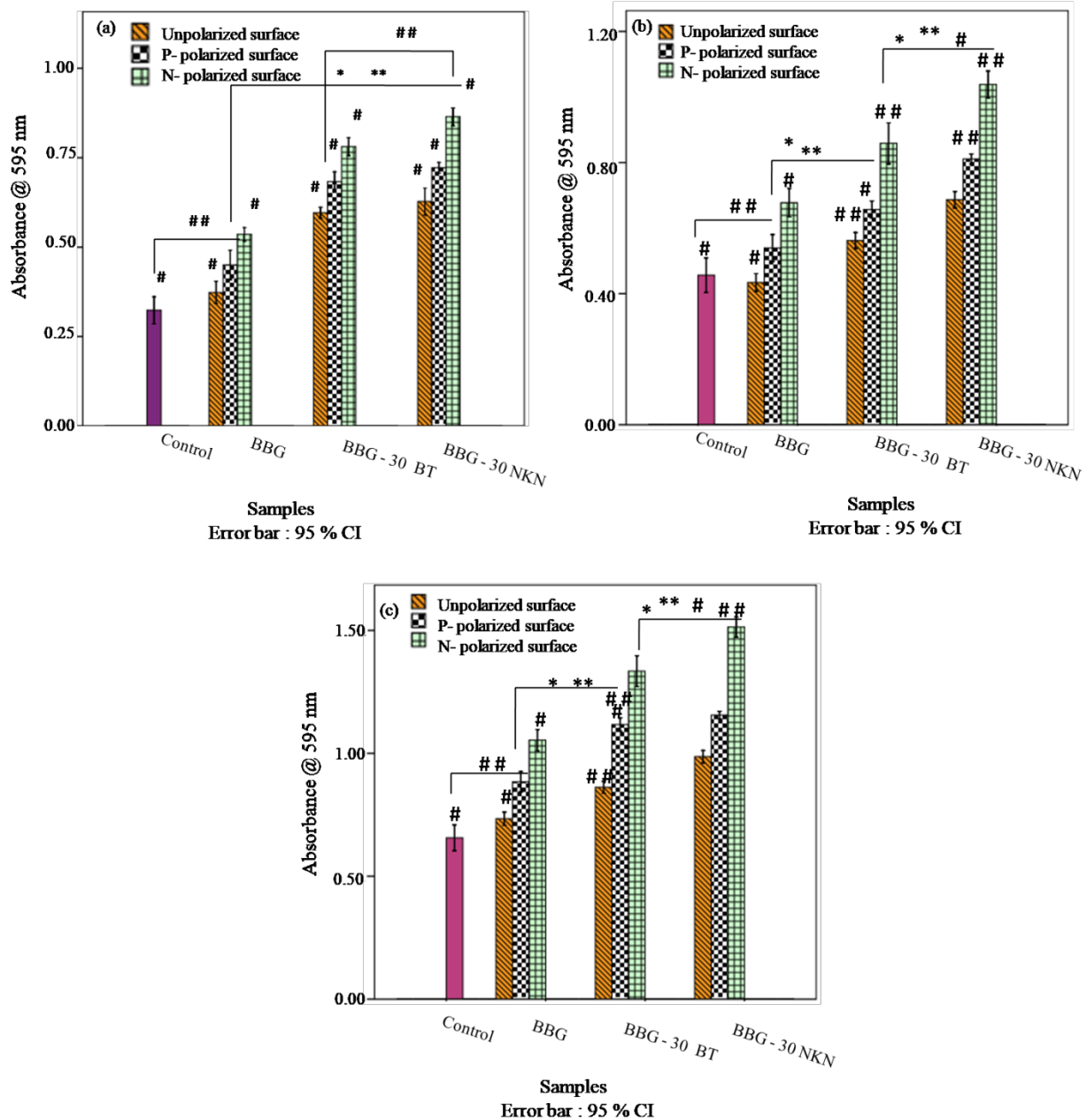
Fig. 6.7. The viability of osteoblast like MG-63 cells, cultured on BBG, and BBG – x BT/NKN (x = 30 vol. %) composites after incubation of (a) 3 (b) 5 and (c) 7 days. The symbols (*) and (**) represent the statistically significant difference among all the samples with respect to control sample (glass cover slip) and unpolarized BBG, respectively, at p < 0.05. The symbols (#) and (##) represent the statistically significant difference among all the samples with respect to P-polarized and N- polarized BBG, respectively, at p < 0.05.

6.3.2. Cell morphology

The morphology of MG-63 cells, adhered on BBG-x (x = 30 vol. %) BT/NKN composite samples were observed using fluorescence microscopic images. Fig. 6.8 represents the morphology of MG-63 cells, adhered on the surface of unpolarized and polarized BBG-x BT/NKN (x = 30 vol. %) composite samples, after 3 days of culture. The density of MG-63 cells increases with incorporation of piezoelectric NKN/BT (30 vol. %) on composite sample surfaces as compared to unpolarized BBG [Fig. 6.8 (a-c)]. Irrespective of addition of secondary phases, the polarized surfaces also enhance the cell density. The negatively polarized surfaces have higher cell density as compared to unpolarized and positively polarized surfaces of the same sample [Fig. 6.8 (d-f)]. The density of adhered MG-63 cells is observed to be maximum on BBG-30 vol. % NKN composite samples [Fig. 6.8 (f)]. Overall, the negatively polarized surfaces have higher cell density as compared to unpolarized and positively polarized surfaces.

It has been reported that BBG releases K^+, Na^+, BO^{3-} and PO_4^{3-} ions after immersion in physiological solution. The presence of Ca^{2+} ions in the media react with released BO^{3-} and PO_4^{3-} ions and start the formation of hydroxyapatite layer [20,21]. In addition, the released ions promote the osteogenic gene expression [22]. It has been observed that proliferation of MG-63 cells increases with incorporation of piezoelectric BT/ NKN as secondary phase. Apart from addition of piezoelectric secondary phases, the polarized substrates also increase the cell viability.
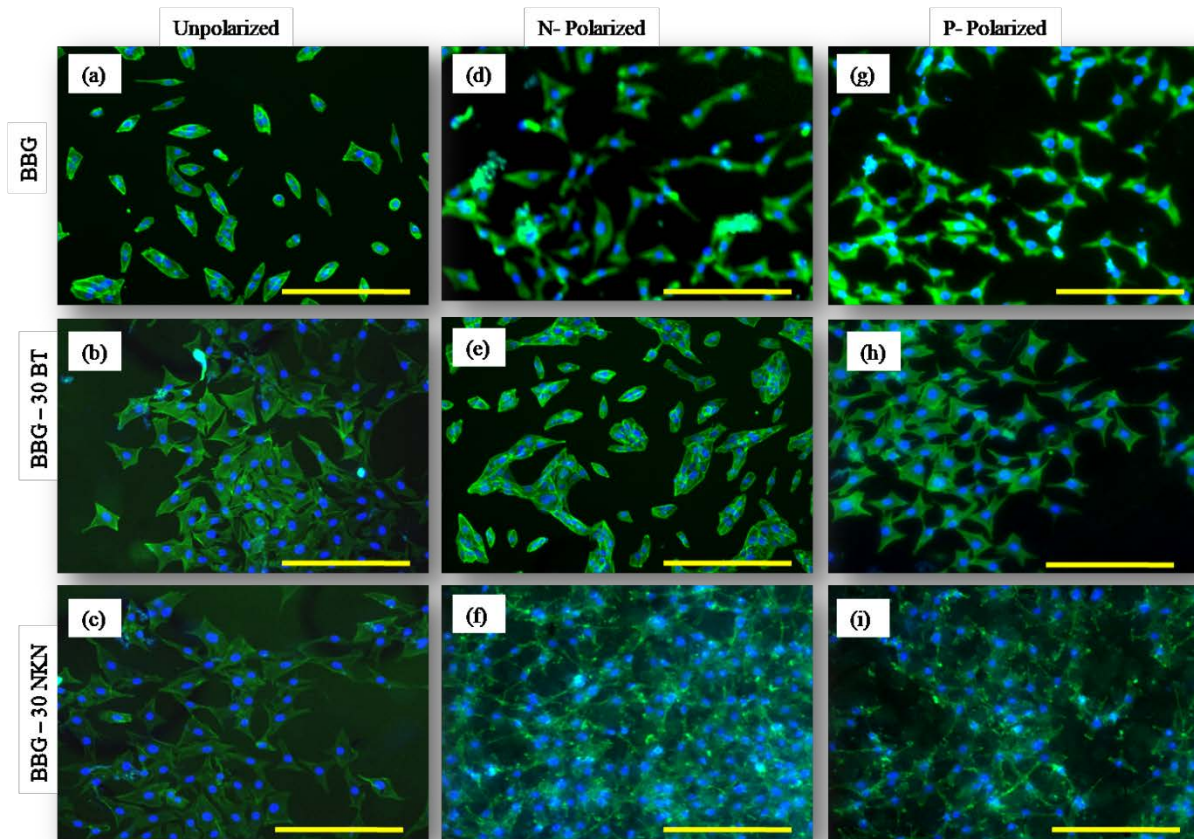
Fig. 6.8. Fluorescence images of MG-63 cells, adhered on unpolarized and polarized surfaces of BBG-x BT/NKN (x = 30 vol. %) composite samples, after incubation of 3 days (scale bars corresponds to 100 μm).

The negatively charged NKN and BT surfaces attract the Ca^{2+} ions present in the media and these ions react with the charged proteins, available in the cell medium and promote the adhesion and proliferation of osteoblast cells [23]. The negatively charged surfaces of HA-30 vol. % BT, and HA-30 vol. % NKN composites demonstrate higher adhesion and proliferation of MG-63 cells [24].

6.4. Closure

The BBG was successfully synthesize using melt quench method and BBG-30 vol. % NKN and BBG -30 vol. % BT composites were prepared using solid state mixing route. The XRD analyses confirm the formation of single phase BBG. The distinct phases of BT and NKN were observed in composite samples. The BBG demonstrates inherent antibacterial property due to presence of boron. The incorporation of piezoelectric BT/ NKN (30 vol. %) in BBG as secondary phase increases the antibacterial response. The adhesion of *E. coli* and *S. aureus* bacteria on negatively polarized surfaces has been reduced due to electrostatic repulsion between charge on bacterial membrane (negative charge) and material surface. On the other hand, negatively charged surfaces promote the adhesion and proliferation of osteoblast like MG-63 cells. Overall, it can be concluded that incorporation of piezoelectric BT/ NKN (30 vol. %) in BBG matrix as well as surface polarization increases the antibacterial and cellular response.

References

1. H.S. Choi, J.W. Kim, Y.N. Cha, C. Kim, A quantitative nitrobluetetrazolium assay for determining intracellular superoxide anion production in phagocytic cells. *Journal of Immunoassay and Immunochemistry*. **27** (2006) 31-44.

2. M.V. Berridge, P.M. Herst, A.S. Tan, Tetrazolium dyes as tools in cell biology: New insights into their cellular reduction Biotech. *Annual Reviews*, **11** (2005) 127-152.

3. J. M. Slauch, How does the oxidative burst of macrophages kill bacteria Still an open question. *Molecular Microbiology.* **80(3)** (2011) 580–583. doi:10.1111/j.1365-2958.2011.07612.x

4 G. Applerot, A. Lipovsky, R. Dror, N. Perkas, Y. Nitzan, R. Lubart, A. Gedanken, Enhanced antibacterial activity of nanocrystalline ZnO due to increased ROS-mediated cell injury. *Advanced Functional Materials*, **19** (2009) 842–852.

5. A.T. Poortinga, J. Smit, H.C. Van der Mei, J.H. Busscher, Electric Field Induced Desorption of Bacteria From a Conditioning Film Covered Substratum. *Biotechnology and Bioengineering*, 76 (2001) 395−399.

6. C. Beauchamp, and I. Fridovich, A Mechanism for The Production of Ethylene From Methional. The Generation of the Hydroxyl Radical By Xanthine Oxidase. *Journal of Biological Chemistry,* **245** (1970) 5214–5222.

7. M. Hamadouche, A. Meunier, D. C. Greenspan, C. Blanchat, J.P. Zhong, G. P. L. Torre and L. Sedel Long-term in vivo bioactivity and degradability of bulk sol–gel bioactive glasses *Journal of Biomedical Materials Research,* **54** (2001) 560–6.

8. M.L. Cooper, J.F. Hansbrough, Use of a composite skin graft composed of cultured human keratinocytes and fibroblasts and a collagen-GAG matrix to cover full-thickness wounds on athymic mice. *Surgery*. **109(2) (**1991) 198-207.

9. W. Huang, M. N. Rahaman, D. E. Day and Y. Li 2006 Mechanisms for converting bioactive silicate, borate, and borosilicate glasses to hydroxyapatite in dilute phosphate solution *Phys. Chem. Glasses: Eur. J. Glass Sci. Technol.* B**47** 647–58

10. O.L.̈ranta, M. Vaahtio, T. Peltola, D. Zhang, L. Hupa, M. Hupa, H. Ylänen, J. I. Salonen, M. K. Viljanen, E. Eerola, Antibacterial effect of bioactive glasses on clinically important anaerobic bacteria in vitro, *Journal of Materials Science: Materials in Medicine*, **19** (2008) 547–551.

11. T. Yao, Ju. Chen, Z. Wang, J. Zhai, Y.Li, J. Xing, S. Hu, G. Tan , S.Qi , Y. Chang, P. Yu, C. Ning, The antibacterial effect of potassium-sodium niobate ceramics based on controlling piezoelectric properties, *Colloids and Surfaces B: Biointerfaces,* 175 (2019) 463-468.

12. T. J. Beveridge, Structures of Gram-negative Cell Walls and Their Derived Membrane Vesicles, *Journal of Bacteriology*, **181** (1999) 4725–4733.

13. E. Kłodzinska, M. Szumski, E. Dziubakiewicz, K. Hrynkiewicz, E. Skwarek, W. Janusz, B. Buszewsk, Effect of zeta potential value on bacterial behavior during electrophoretic separation, *Electrophoresis* **31** (2010) 1590–1596.

14. R. Sonohara, N. Muramatsu, H. Ohshima, T. Kondo, Difference in Surface Properties between Escherichia coli and Staphylococcus aureus as Revealed by Electrophoretic Mobility Measurements. *Biophysical chemistry,* **55** (1995) 273-7.

15. M.T. Ehrensberger, M.E. Tobias, S.R. Nodzo, , L.A. Hansen N.R. Luke-Marshall, L.M.; Cole, R.F. Wild, A.A. Campagnari,. Cathodic Voltage-Controlled Electrical Stimulation of Titanium Implants as Treatment for Methicillin-Resistant Staphylococcus Aureus Periprosthetic Infections, *Biomaterials*, **41** (2015) 97-105.

16. G. Harkes, J. Feijen, J. Dankert, Adhesion of Escherichia coli on to a series of poly (methacrylates) differing in charge and hydrophobicity, *Biomaterials,* **12** (1991) 853-860.

17. Y. Liu, R. Qin, S.A.J. Zaat, E. Breukink, M. Heger, Antibacterial photodynamic therapy: overview of a promising approach to fight antibiotic-resistant bacterial infections, *Journal of Clinical Translational Research,* **1(3)** (2015) 140-167.

18. S. Kumar, R. Vaish, and S. Powar, Surface-selective bactericidal effect of poled ferroelectric materials, *Journal of Applied Physics,* **124** (2018).

19 A.K. Dubey, B. Basu, Pulsed Electrical Stimulation and Surface Charge Induced Cell Growth on Multistage Spark Plasma Sintered Hydroxyapatite Barium Titanate Piezobiocomposite, *Journal of the American Ceramic Society.* **97** (2014) 481–489.

20. G. R. Li, H. Sun, X. Deng, C. P. Lau Characterization of ionic currents in human mesenchymal stem cells from bone marrow. *Stem Cells,* **23** (2005) 371–382.

21. F Ding, G. Zhang, L. Liu, L. Jiang, R. Wang, Y. Zheng, G. Wang, M. Xie, Y. Duan. Involvement of cationic channels in proliferation and migration of human mesenchymal stem cells. *Tissue and Cell,* **44 (**2012) 358–364.

22. M. Ohgaki, T. Kizuki, M. Katsura, K. Yamashita, Manipulation of selective cell adhesion and growth by surface charges of electrically polarized hydroxyapatite. *Journal of Biomedical Materials Research,* **57 (**2001) 366–373.

23. C.J. Wilson, R.E. Clegg, D.I. Leavesley, M.J. Pearcy, Mediation of biomaterial–cell interactions by adsorbed proteins: A review. *Tissue Engineering*, **11** (2005) 1–18.

24. K. S. Hwang, J. E. Song, H. S. Yang, Y. J. Park, J. L. Ong, and H. R. Rawls, "Effect of Poling Conditions on Growth of Calcium Phosphate Crystal in Ferroelectric BaTiO$_3$ Ceramics," *Journal of Materials Science: Materials in Medicine*, **13** (2002) 133–8.